

Unbiased Scene Graph Generation via Rich and Fair Semantic Extraction

Bin Wen, Jie Luo, Xianglong Liu

State Key Laboratory of Software Development Environment,
School of Computer Science and Engineering, Beihang University
No. 37, Xueyuan Road, Beijing 100191, P.R. China

{wenbin,luojie,xlliu}@nlsde.buaa.edu.cn

Lei Huang

Inception Institute of Artificial Intelligence (IIAI)

Abu Dhabi, UAE

lei.huang@inceptioniai.org

Abstract

Extracting graph representation of visual scenes in image is a challenging task in computer vision. Although there has been encouraging progress of scene graph generation in the past decade, we surprisingly find that the performance of existing approaches is largely limited by the strong biases, which mainly stem from (1) unconsciously assuming relations with certain semantic properties such as symmetric and (2) imbalanced annotations over different relations. To alleviate the negative effects of these biases, we proposed a new and simple architecture named Rich and Fair semantic extraction network (RiFa for short), to not only capture rich semantic properties of the relations, but also fairly predict relations with different scale of annotations. Using pseudo-siamese networks, RiFa embeds the subject and object respectively to distinguish their semantic differences and meanwhile preserve their underlying semantic properties. Then, it further predicts subject-object relations based on both the visual and semantic features of entities under certain contextual area, and fairly ranks the relation predictions for those with a few annotations. Experiments on the popular Visual Genome dataset show that RiFa achieves state-of-the-art performance under several challenging settings of scene graph task. Especially, it performs significantly better on capturing different semantic properties of relations, and obtains the best overall per relation performance.

1. Introduction

Extracting explicit semantic representation from images is one of the main challenges in computer vision. Recently,

there has been increasing interest on using scene graph [6] as representation, in which objects in the image are represented as vertices and relations between objects are represented as edges. From the perspective of knowledge, a scene graph can be viewed as a kind of knowledge graph, where objects are corresponding to entities, classes of objects are corresponding to classes of entities, and relations are corresponding to object properties between entities.

In the past decade, there has attracted a number of studies that attempted to generate the scene graph using various techniques. There are mainly two types of methods for scene graph generation. The first type concentrates on utilizing internal information such as the visual features of images. Typical techniques include iterative message passing [22], associative embeddings [15], graph neural network [23, 21]. The second type tries to combine internal information and external knowledge such as language features and knowledge graphs. Typical techniques include motifs [24], knowledge distillation [17], knowledge embedding [26]. Unfortunately, in practice these methods often learn the biased models for scene graph generation, mainly due to the incorrect assumption of relations properties and the imbalanced annotations in the training set.

First, most of these methods treat the relations as the labels, usually based on the biased assumption that the relations among entities follow certain semantic properties like symmetry between the subject and object. In fact, the scene graph is a formal representation of knowledge, where relations are not just labels for classifying pairs of entities, but own specific semantic properties that serves as a meta constraint defining the exact meanings of the relations (see examples in Figure 1). Second, the imbalanced annotations for different relations lead the trained models to mainly focus on the frequent relations, and inevitably generates

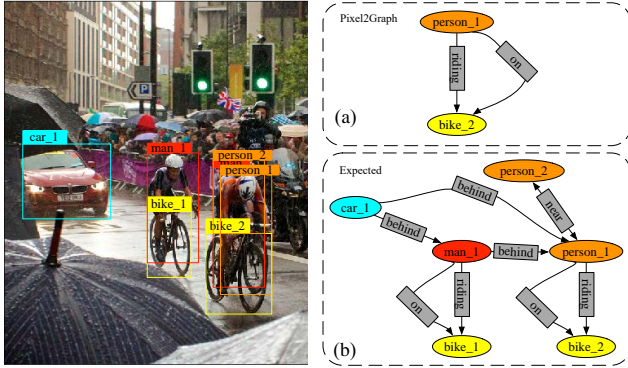


Figure 1. An example of relations with different properties. (a) is the scene graph generated by the Pixel2Graph model [15]; although its prediction matches the ground truth, there are still many relations and their properties not being recognized as shown in (b). For example, relation “riding” is asymmetric, i.e. if (man_1, riding, bike_1) is a relation instance, then its symmetric form (bike_1, riding, man_1) is not a relation instance; relation “near” is symmetric, i.e. if (person_1, near, person_2) is a relation instance, then (person_2, near, person_1) is also a relation instance; relation “behind” is transitive, i.e. if (car_1, behind, man_1) and (man_1, behind, person_1) are both relation instance, then (car_1, behind, person_1) is also a relation instance. These semantic properties of relations are reflected by the triples that constitute the scene graph.

the biased prediction ignoring those uncommonly occurred ones, which may be very valuable in applications such as medical diagnosis. The imbalanced relations can be often observed in the widely used datasets for scene graph task [2, 26], such as Visual Genome.

To avoid the two kinds of biases, we propose the Rich and Fair semantic extraction network (RiFa), a novel architecture designed to not only reveal the rich semantic properties of relations, but also fairly extract relations with different annotation intensity. Specifically, we devise a pseudo-siamese network for independently embedding entities into separate subject and object feature vectors. The feature representation can distinguish the semantic difference between subject form and object form of the same entity, and thus avoids implicitly imposing constraints or biases on relations, which usually happens in traditional methods. Moreover, to fairly handle relations with different annotation intensities, the relations of a subject-object pair are predicted based on both the embeddings of subject-object pair and the contextual visual features extracted from the smallest bounding box covering both entities in the pair. Then, a relation score that does not depend on the statistical distribution of annotations is devised to rank all possible predictions and promote the true relations, even with a few annotations.

Extensive experiments on the Visual Genome [7] dataset show that RiFa not only achieves the state-of-the-art standard recall performance on several task settings comparing to previous approaches, but also has the best overall

per relation performance. The RiFa model also demonstrates significantly better performance on capturing different semantic properties. Note that our method only relies on the simple convolutional neural network, but can obtain the state-of-the-art performance, compared to those sophisticated methods such as graph neural network based ones. This means that the principle behind our design that eliminates the biases provides a new sight to the study of scene graph generation.

2. Related Work

There are many ways to formulate the task of extracting relations between entities in images. Visual relation detection (VRD) [13] and scene graph generation [6] are two common tasks that attract the attention of many researchers recently for the challenging nature of the tasks and the complexity of the corresponding datasets used for training.

For visual relation detection, the current works are mainly focus on capturing interactions between object pairs [14, 18, 16]. For scene graph generation, the approaches can be divided into two types based on whether they utilize external knowledge [10, 25, 21].

Scene Graph Generation Based on Visual Features. The DR-Net models the scene graph generation as inference on a conditional random field (CRF) [3]. [22] uses Recurrent Neural Network (RNN) for relation extraction and message passing for improving predictions iteratively. [15] propose a end-to-end scene graph extraction approach based on associative embeddings to predict relations using heatmap. Qi et al propose an attentive relational network for mapping images to scene graphs [19].

To improve the scalability of models, [8] tries to tackle the problem of the quadratic combinations of possible relationships by introducing a concise subgraph-based representation of the scene graph. [23] proposes a scene graph generation model based on Graph R-CNN, which uses a relation proposal network to deal with the quadratic number of potential relations between objects. Our model also use an approach that is similar in spirit to the above two for filtering subject-object pairs. However, our model uses a measurement learned through data to predict the likelihood of a subject-object pair having relations.

To handle the imbalanced annotations of relations, [2] builds a graph representation of statistical correlations between object pairs and their relationships, and uses a graph neural network to learn the interplay between relationships and objects to generate scene graph.

Scene Graph Generation Based on External Knowledge. [13] combines visual and language features for relation detection of object pairs. [24] utilizes the statistical information about repeated motifs in the datasets and global context to predict all possible relations between pairs of objects. [9] uses region captions to provide context for scene

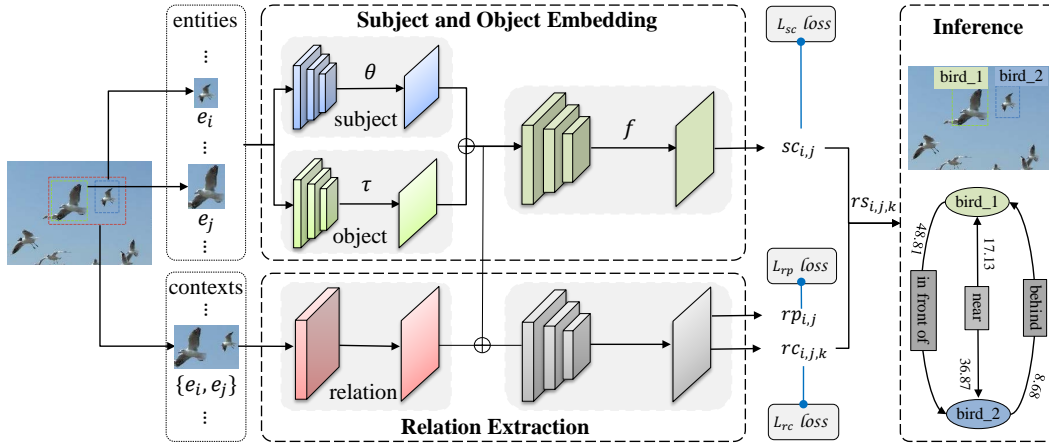


Figure 2. The overall pipeline of the RiFa model.

graph generation. [17] incorporates knowledge distillation into neural network to improve the prediction. [26] joints visual features from images and semantic features from external knowledge bases to handle imbalanced distribution of triples.

Unlike many of the above approaches that only treat the scene graph task as labeling entities and relations between entities, our model tries to extract richer semantics including relations between entities with specific semantic properties and alleviate the imbalance between different relations by eliminating biases.

3. The RiFa Model

In this paper, we argue that the performance bottleneck of most existing scene graph generation methods largely stems from the unexpected biases in both the unreasonable assumption of relation properties and the imbalanced relation annotations. Therefore, our goal is to generate more accurate scene graph by utilizing this clue and a simple conventional convolutional network architecture. We propose the Rich and Fair semantic extraction network (RiFa), which treats the scene graph generation as a process of extracting knowledge graph, and is able to extract richer semantics and preserve the fairness for relations with imbalanced distributions.

The overall pipeline of our RiFa model is shown in Figure 2. As the figure shows, given an image, the RiFa model first extracts the visual feature maps with a backbone. Then, each entity e_i in the image is embedded into subject and object feature vectors $\theta(e_i)$ and $\tau(e_i)$ separately from its visual feature obtained by ROI align on feature maps, entity class, and bounding box through a pseudo-siamese network. Semantic connection strength $sc_{i,j}$, the likelihood of whether a subject-object pair (e_i, e_j) has relations, is predicted by passing subject and object embeddings through a three layers fully-connected neural network

(FCN). The top- N pairs that are most likely to have relation are passed for further relations extraction. The relations $rc_{i,j,1}, \dots, rc_{i,j,n}$ between subject-object pair (e_i, e_j) as well as the possibilities $rp_{i,j}$ that the pair has relations are predicted based on relation (context), subject, and object features, where n is the number of relation classes. Finally, the resulting triples are sorted based on relation score $rs_{i,j,k}$ computed from $sc_{i,j}$, $rp_{i,j}$, and $rc_{i,j,k}$, and the top- k triples are selected as the final result of relation extraction.

3.1. Rich Subject and Object Semantic Embedding

In existing scene graph generation models, they usually embed every entity e into a vector through the same projection function σ . However, an entity has notable differences visually and semantically when it is used as subject and object in a relation. Ignoring such difference may have negative impact on capturing semantic properties of relations such as asymmetry. To address the assumption bias, this paper converts the visual entities into semantically different subjects and objects features separately through two projection θ and τ , which are learned through a pseudo-siamese network whose two branches are the same convolutional neural network without sharing parameters. In such a way, every visual entity e is represented by independent subject embedding $\theta(e)$ and object embedding $\tau(e)$ simultaneously.

The two branches of the pseudo-siamese network for subject and object entity embedding have the same structure as the one described in Figure 3. The inputs of the network are one hot embedding of entity class (or the predicted class vector in case of when the entity class is not provided), entity bounding box, and feature vector obtained by ROI align [4] on visual feature maps.

In order to produce the correct subject-object pairs passed to relation prediction, we introduce a binary classifier for filtering out pairs that are unlikely to have relations, which require a metric for measuring likelihood that

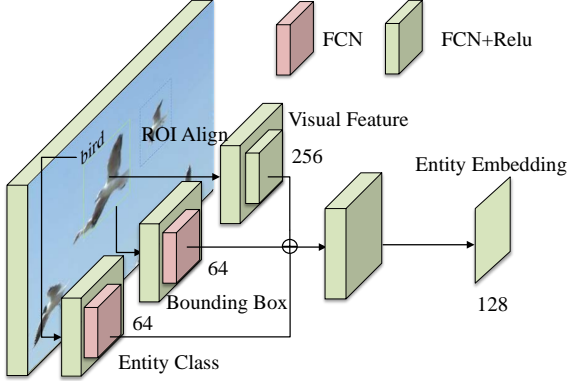


Figure 3. The network structure for entity embedding.

a subject-object pair has reasonable relations. However, common measurements such as cosine (angular) distance or Gaussian distance have both symmetry and triangle inequality properties, which may introduce bias that forces relations to become symmetric and/or transitive. For a general relation, it is not necessarily to have properties such as symmetry or transitivity. Hence, we define a new measurement named *semantic connection strength*.

The semantic connection strength of a subject-object pair (e_i, e_j) is defined as

$$sc_{i,j} = f(\theta(e_i), \tau(e_j)), \quad (1)$$

where $\theta(e_i)$ and $\tau(e_j)$ are the subject embedding of e_i and object embedding of e_j , and f is a function learned by passing the concatenation of subject and object embeddings through a three layers FCN with activation function \tanh to map the result to $[-1, 1]$. When $sc_{i,j}$ is approaching 1, it means that the i th entity e_i and the j th entity e_j are more likely to have relations; otherwise, it means they are less likely to have relations.

Because the subject-object pairs which have relations are usually only 10% of all pairs, so when defining the semantic connection loss based on the classic cross-entropy, the model cannot achieve expected performance. Thus, we further introduce a *semantic connection loss* L_{sc} for training the pseudo-siamese network. It uses an addition penalty term to compensate the bias caused by the massive pairs that have no relations, which is defined as the average cross-entropy of all subject-object pairs that have relations. For an image containing m entities, let us denote the set of indexes of subject-object pairs which have relations as I_t and the remaining set as I_f according to the ground truth. It is obvious that $|I_t| + |I_f| = m^2$. Let

$$\delta_{i,j}^C = \begin{cases} 1, & (i,j) \in C \\ 0, & \text{otherwise} \end{cases}. \quad (2)$$

The semantic connection loss is defined as follows.

$$L_{sc} = \sum_{i,j \in [1,m]} -\lambda_{i,j} \cdot \ln \left(\frac{1 - (-1)^{\delta_{i,j}^{I_t}} sc_{i,j}}{2} \right), \quad (3)$$

where

$$\lambda_{i,j} = \frac{1}{m^2} + \frac{\delta_{i,j}^{I_t}}{|I_t|}. \quad (4)$$

Here $\frac{1}{m^2}$ is the weight for obtaining the classic cross-entropy, while $\frac{\delta_{i,j}^{I_t}}{|I_t|}$ is the weight for addition reward to compensate the imbalance between pairs that have relation and those do not.

With the pseudo-siamese network, for a given image with m entities, we can select the subject-object pairs with top- N highest semantics connection strength for further relation prediction from the m^2 possible combinations.

3.2. Fair Extraction of Imbalanced Relations

As aforementioned, in practice the annotations for different relations are quite imbalanced. For example, in the Visual Genome dataset about 76% of the ground truth annotations are triples about only 5 relations: “wearing, has, on, of, in”. As a result, the relations that frequently occur in images are easy to extract and dominates the model predictions with a strong bias, while the relations that only occur in a small number of images are hard to extract, especially for frequency based approaches. In order to make the relation extraction more fair for different types of relations, we predict relations between two entities by combining their subject and object entity embedding with relation embedding, and the possibility that the subject and object entities have relations simultaneously.

In order to define the relation embedding, we first define the relation bounding box for a relation instance as the smallest rectangle which covers the bounding boxes of both its subject and object. The relation embedding is the visual feature within the relation bounding box in the image, which describes the context of relations between the two entities. Besides, the combination of relation embedding with the subject and object entity embeddings can also help to solve the problem that multiple subject-object pairs have overlapping relation bounding boxes. It also support the case that a single subject-object pair has multiple relations.

To accurately filter out subject-object pairs which do not have relations, the *relation possibility* $rp_{i,j}$ is predicted simultaneously with the relation classes to measure the possibility that the i th subject and the j th object have relations. We introduce *relation possibility loss* L_{rp} to guide the learning of the relation extraction network, in which a penalty term similar to the one defined in L_{sc} is used.

Formally, for the N subject-object pairs proposed for further prediction, let us denote the index set of subject-

object pairs as E , those have relations as E_t and the remaining set as E_f according to the ground truth. We have $|E_t| + |E_f| = N$ and $|E_t| \leq |I_t|$. The relation possibility loss L_{rp} is defined as follows.

$$L_{rp} = \sum_{(i,j) \in E} -\gamma_{i,j} \cdot \ln \left(\text{rp}_{i,j}^{\delta_{i,j}^{E_t}} (1 - \text{rp}_{i,j})^{(1 - \delta_{i,j}^{E_t})} \right), \quad (5)$$

where

$$\gamma_{i,j} = \frac{1}{N} + \frac{\delta_{i,j}^{E_t}}{|E_t|}. \quad (6)$$

Similar to the case of $\lambda_{i,j}$, $\frac{1}{N}$ is the weight for obtaining the classic cross-entropy, while $\frac{\delta_{i,j}^{E_t}}{|E_t|}$ is the penalty term.

3.3. Training and Inference

Training. The final module of the RiFa model is to predict relations between subject-object pairs. For the training of relation prediction, we define the *relation class loss* L_{rc} , in which we only need to consider the subject-object pairs that have relations. So the relation class loss can be defined as the cross-entropy of all relations in the subject-object pairs which have relations. Let us denote the index set of relations between the i th subject and the j th object as $R_{i,j}$ and $r = \sum_{(i,j) \in I_t} |R_{i,j}|$. Then, since there can be more than one relation between the same subject-object pair, $r \geq |I_t|$. The relation class loss L_{rc} is defined as follows.

$$L_{rc} = \frac{1}{r} \sum_{(i,j) \in I_t} \sum_{k \in R_{i,j}} -\ln(\text{rc}_{i,j,k}), \quad (7)$$

where $\text{rc}_{i,j,k}$ is the possibility that the relation between the i th subject and the j th object is the k th relation.

The loss function for RiFa is defined as

$$L = L_{sc} + L_{rp} + L_{rc}, \quad (8)$$

where the above three losses are weighted equally.

Inference. Based on the above description of the RiFa model, three kind of values can be produced in the inference: semantic connection strength $sc_{i,j}$, relations possibility $\text{rp}_{i,j}$, and relation classes map $\text{rc}_{i,j}$ which constitutes by the possibility of the relation between i th subject and j th object belonging to each relation classes. Based on these values, we propose the following *relation score* $\text{rs}_{i,j,k}$ to systematically represent the likelihood that the i th subject and the j th object have the k th relation.

$$\text{rs}_{i,j,k} = sc_{i,j} + \beta \cdot \text{rp}_{i,j}^2 \cdot \text{rc}_{i,j,k}, \quad (9)$$

where β is a parameter for tuning the weight of different scores. The semantic connection strength is the core part of the relation score, which distinguishes subject-object pairs

that do have relations with those do not. The relation possibility can be viewed as a refinement of the semantic connection strength, which more accurately reflects the possibility that a subject-object pair have relations and can alleviate the negative impact of the false-positives in the top- N subject-object pairs. It can also benefit subject-object pairs that have multiple relations by lowering the ranks of triples that are not instances of relations and increasing the ranks of triples that reflect different relations between the same subject and object. Because it is very common in datasets such Visual Genome that there are multiple relations between the same subject-object pair, it can increase the chance that relations with only a few annotations to be extracted with a higher relation scores.

The advantage of this definition is that it does not depend on statistical distribution of relation instances. So both relations with a large number of annotations and those with only a few have relatively equal chance to be ranked in the top- k predictions.

Implementation. We implement and train the RiFa in TensorFlow [1]. RiFa takes a 512x512 image for input and outputs a vector to indicate the predicted relation. The visual feature maps of images are extracted first, which contain visual features of all entities and relations between entities. Because the size of entities in images is variant, it is difficult to capture the visual and semantic features of entities with different size. Thus, to archive precise object classification and relation extraction, we draw inspiration from Feature Pyramid Network (FPN) [11] to generate both 32×32 and 16×16 feature maps to obtain visual information of different granularity after extracting visual features through a VGG19 network. Unlike the FPN model which utilize different feature map separately, we combine them together for future usage.

4. Experiments and Evaluations

4.1. Experiment Settings

All the experiments are performed on a workstation with two GeForce GTX 1080Ti GPUs, which has Ubuntu 18.04 operation system, CUDA 9.0, CUDNN 7.0, and TensorFlow 1.8. For the hyper-parameters, we set $\beta = 120$ and $N = 100$ across all experiments.

Dataset. The performance of RiFa is evaluated on Visual Genome, using the publicly available preprocessed version with 150 classes and 50 relations (VG150) and the same split by [22].

Task Setting. The task of scene graph generation is to produce a set of triples of form (s, p, o) , where the subject s is an entity in the image defined by its bounding box, the object o can be an entity or a class. In case that o is a class, (s, p, o) represents that the entity s is an instance of class o ; otherwise, p is a relation between two entities in the im-

	SGCls		PredCls	
	R@50	R@100	R@50	R@100
VRD	11.80	14.10	27.90	35.00
IMP	21.72	24.38	44.80	53.00
Pixel2Graph	26.5	30.0	68.0	75.2
GPSKD	35.55	42.74	67.71	77.60
MotifNet	35.8	36.5	65.2	67.1
Graph R-CNN	29.6	31.6	54.2	59.1
LSVRU	36.7	36.7	68.4	68.4
CISC	27.8	29.5	53.2	57.9
RiFa	37.62	44.38	80.64	88.35

Table 1. Comparison results for SGCls and PredCls tasks.

age. A triple is correct according to the ground truth, if the classes of entities and relations between entities match those of ground truth. Following [22] and [15], this paper uses the standard evaluation metric $R@k$ for scene graphs, which measures the percentage of ground truth triples in the set of top- k proposals. The performance of RiFa on the following three tasks are evaluated: 1) **PredCls**: given an image, bounding boxes, and classes of entities defined by the bounding boxes, predicting relations between entities; 2) **SGCls**: given an image and bounding boxes for entities in the image, predicting the classes of entities and relations between entities; 3) **SGGen**: given an image only, predicting the classes of entities and relations between entities.

4.2. Comparison to State of the Art

We first evaluate our RiFa on the Visual Genome dataset with comparison to state-of-the-art methods, including VRD [13], IMP [22], Pixel2Graph [15], GPSKD [17], MotifNet [24], Graph R-CNN [23], LSVRU [26], and CISC [21]. In order to perform the SGCls task with RiFa, we extend the model of RiFa with an auxiliary network for entity classification after predicting the relations between a subject-object pair. The entities are classified not only based on their own embeddings but also relations between entities. During the evaluation, both SGCls and PredCls tasks are conducted with RiFa alone. The comparison results on the above three tasks are listed in Table 1.

For the $R@100$ metric, RiFa archives the state-of-the-art performance on the PredCls and SGCls tasks. For the $R@50$ metric, RiFa archives the best performance on the PredCls task and has a performance comparable to that of state-of-the-art approaches on the SGCls task.

For the SGGen task, we report the results in Table 2 for the sake of completeness by combining RiFa with bounding boxes and entity classes detected by a Faster R-CNN [20] with ResNet-101 [5], which is pre-trained with the COCO dataset [12] and fine-tuned on the Visual Genome dataset. RiFa still has a reasonably good performance on it com-

paring to other approaches. We believe RiFa can perform better with a better object detector and more fine-tuning. The models in [24] and [26] achieve a better performance mainly because they either utilize the statistical clue from the dataset or introduce external knowledge base. In models that generate scene graphs without such prior information, e.g. Pixel2Graph, Graph R-CNN, CISC, our RiFa model achieves better performance for both $R@50$ and $R@100$.

4.3. Ablation Study

We explore 3 settings of the RiFa models to verify the effectiveness of the network for relation prediction: 1) the one without relation embedding (RE), 2) the one without subject and object embeddings (SOE), 3) the one without relation possibility (RP). The intuition of concatenating relation embedding with subject and object embeddings is that the latter contains both visual and semantic features of the entities in the subject and object, while the former provides the context information about the relation between these two entities, and these two features are complementary.

As shown in Table 3, the combination of relation embedding with subject and object embeddings outperforms models that with only one feature by a large margin, which demonstrates the efficacy of the concatenation. The relation possibility is designed to reduce false-positives by lowering the relation score of entities that actually have no relations. The experiment result indicates that by incorporating relation possibility in to the relation extraction network, the performance is clearly improved.

	R@50	R@100
VRD	0.30	0.50
IMP	3.40	4.20
Pixel2Graph	6.70	7.80
MotifNet	27.2	30.3
Graph R-CNN	11.4	13.7
LSVRU	27.9	32.5
CISC	11.4	13.9
RiFa	20.86	26.68

Table 2. Comparison results for the SGGen task.

	PredCls	
	R@50	R@100
RiFa	80.64	88.35
RiFa w/o RE	60.43	71.33
RiFa w/o SOE	45.12	61.84
RiFa w/o RP	77.32	85.88

Table 3. Ablation study of RiFa.

	Pixel2Graph	RiFa
$R_A@50$	65.33	84.41
$R_A@100$	53.02	84.34
$R_S@50$	35.84	15.53
$R_S@100$	48.92	29.65
$R_I@50$	11.48	8.05
$R_I@100$	29.34	22.16

Table 4. The performance of Pixel2Graph and RiFa on capturing asymmetry, symmetry, and inverse properties.

4.4. Unbiased Scene Graph Generation

4.4.1 Performance on Capturing Semantic Properties

We conduct experiments on comparing the ability of different neural networks on capturing asymmetry, symmetry, and inverse properties of relation, because they are the most common properties for relations in Visual Genome. The asymmetric relations “wearing, has, riding, on, holding, parked on, walking on”, symmetric relations “and, near”, and mutually inverse relation pairs “(in front of, behind), (above, under), (has, part of)” are chosen for the evaluation. Let us denote the set of top- k predictions for the PredCls task as P_k . We modify the definition of whether a triple in P_k matches the ground truth for the three groups of relations as follows.

Asymmetry. Let p be an asymmetric relation. If $(s, p, o) \in P_k$ matches the ground truth and $(o, p, s) \notin P_k$, then (s, p, o) matches the ground truth w.r.t. asymmetry property.

Symmetry. Let p be a symmetric relation. If $(s, p, o) \in P_k$ matches the ground truth and $(o, p, s) \in P_k$, then (s, p, o) matches the ground truth w.r.t. symmetry property.

Inverse. Let p and q are inverse to each other. If $(s, p, o) \in P_k$ matches the ground truth and $(o, q, s) \in P_k$, then (s, p, o) matches the ground truth w.r.t. inverse property.

The recalls for the three groups of asymmetric, symmetric, and mutually inverse relations based on corresponding matches defined in above are denoted as $R_A@k$, $R_S@k$, and $R_I@k$ respectively. The three recalls of Pixel2Graph and RiFa on VG150 are listed in Table 4.

We can see that the Pixel2Graph model has low $R_A@k$ values and unusually high $R_S@k$ values, which indicates that it may contain bias that prefers to treat relations as symmetric. As a result, the Pixel2Graph model does not perform well on capturing asymmetry property of relations. The RiFa model has low $R_S@k$ and $R_I@k$ values. By analyzing the annotations of VG150, we find that there are only a few annotations that reflect the symmetry and inverse properties, which may be the cause of the low performance of RiFa on symmetric and mutually inverse relations.

To verify this, we construct the VG+50%/VG+100%

dataset by automatically extending 50%/100% annotations about the above chosen symmetric and mutually inverse relations with their symmetric or inverse forms. For instance, (o, p, s) is added as a new annotation if (s, p, o) is a annotation and p is symmetric, and (o, q, s) is added as a new annotation if (s, p, o) is a annotation and q is inverse to p .

As shown in Table 5, on these two extended datasets, the $R_S@k$ and $R_I@k$ values of RiFa model become comparable to or even significantly higher than those of Pixel2Graph model, which provides support to our conjecture.

With the addition annotations, RiFa performs significantly better than Pixel2Graph on capturing asymmetry and inverse properties and has comparable performance on capturing symmetry property despite the advantage given by the bias of Pixel2Graph model.

4.4.2 Performance on Handling Imbalanced Relations

There are 34 relations in VG150 that have a very small number of annotations (less than 0.5% of all annotations).

From Table 6, we can see that the top-15 list of RiFa contains more relations (40%) with a small number of annotations, which indicates that the RiFa performs better on

		Pixel2Graph	RiFa
VG+50%	$R_S@50$	43.72	33.47
	$R_S@100$	58.11	52.10
	$R_I@50$	58.59	61.31
	$R_I@100$	72.96	77.62
VG+100%	$R_S@50$	44.86	36.44
	$R_S@100$	59.39	56.04
	$R_I@50$	62.56	69.48
	$R_I@100$	73.47	81.34

Table 5. The performance after extending the dataset.

RiFa		Pixel2Graph		MotifNet	
Relation	R@100	Relation	R@100	Relation	R@100
wearing	96.78	on	86.15	wearing	97.55
has	93.05	wearing	86.14	on	95.18
riding	92.75	has	85.10	has	93.57
on	92.19	of	81.03	of	90.36
of	89.45	riding	78.26	riding	89.70
holding	87.81	holding	77.73	holding	83.96
<u>parked on</u>	86.64	wears	77.62	wears	80.72
<u>walking on</u>	83.46	in	73.13	in	79.70
in	80.92	near	69.51	<u>walking on</u>	75.89
sitting on	76.33	with	68.86	<u>sitting on</u>	70.42
wears	74.41	above	68.76	behind	68.89
eating	71.89	sitting on	68.15	near	67.94
<u>carrying</u>	70.51	carrying	65.91	<u>carrying</u>	67.91
<u>laying on</u>	68.56	behind	65.39	with	66.38
<u>at</u>	66.22	<u>under</u>	64.52	<u>parked on</u>	64.30

Table 6. Top-15 per relation performance. Relations with a very small number of annotations are labeled with underline.

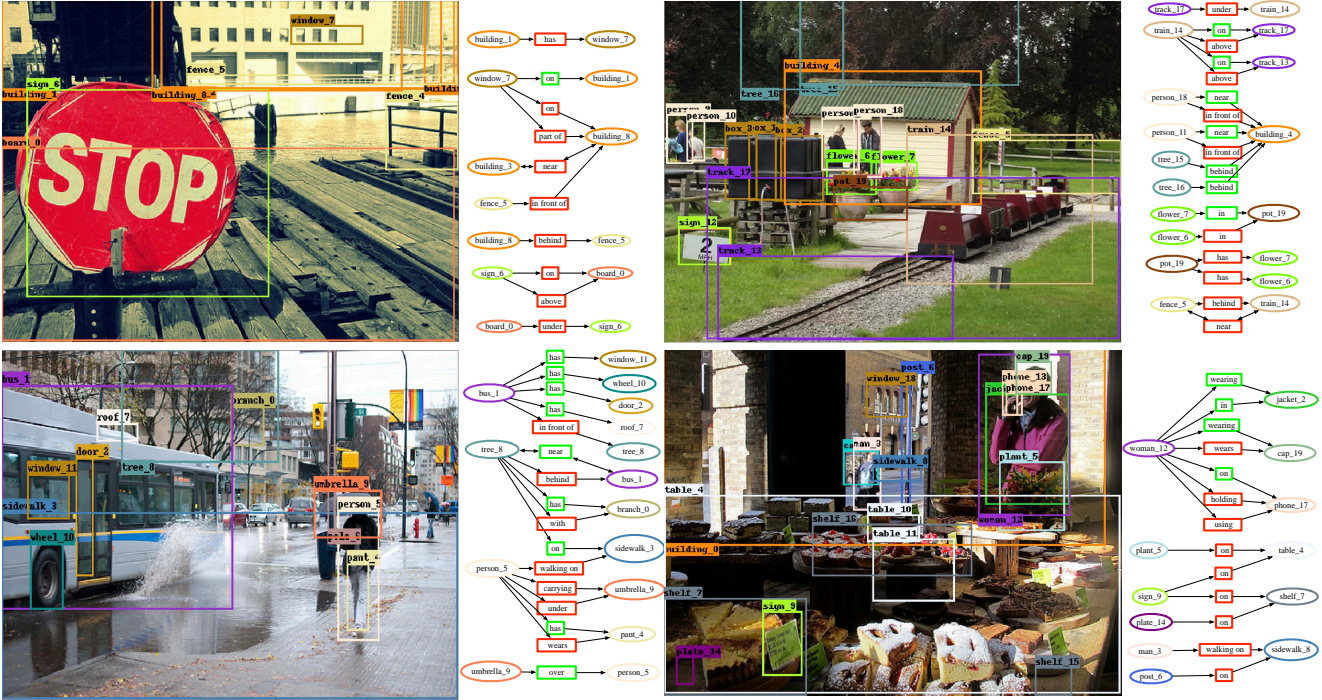


Figure 4. Qualitative examples of relation prediction. Relations outlined in green correspond to triples that match ground truth. Relations in red are correct instances that are not been annotated in the VG150 dataset.

learning to predict not only relations with a large number of annotations but also relations with only a few annotations.

In Figure 5, we can see that the Pixel2Graph model has the smallest number of relations whose per relation $R@100$ values are higher than 80%. While the MotifNet model leads to lower per relation recall for a large number of relations which are mostly relations with relatively small number of annotations. The overall per relation recalls of our RiFa model are consistently better than the other two models. In addition, the mean per relation recall $R@100$ of all 50 relations is 41.61% for the Pixel2Graph model, 37.79% for the MotifNet model, and 48.86% for the RiFa model. Hence, both evidences indicate that our RiFa model has better per relation performance and is more fair for relations

with different scale of annotations.

4.5. Qualitative Results

As shown in Figure 4, our RiFa model is able to extract relations with only a few annotations, such as “walking on”, “carrying”, “over”, “using”. It also demonstrates the ability to capture semantic properties of relations such as asymmetry, symmetry and invert. For example, “walking on” is always predicted to be asymmetric. The two triples (tree.8, near, bus_1) and (bus_1, near, tree.8) are both predicted for the bottom left image, which is a reflection that “near” relation is symmetric. Mutually inverse relation pairs, such as (has, part of), (in front of, behind), (above, under), are also been correctly recognized by RiFa.

5. Conclusion

This paper presented a new model design principle for improving the performance of scene graph generation, i.e. avoiding two types of biases in models: assumptions about semantic properties of relations such as symmetry and imbalanced annotations for different relations. Based on this principle, the RiFa model was proposed to not only capture rich semantic properties of relations, but also fairly extract relations with different annotation intensity. Experimental results shown that the RiFa model achieved the state-of-the-art performance on several tasks comparing to other sophisticated methods, even though it only relies on simple convo-

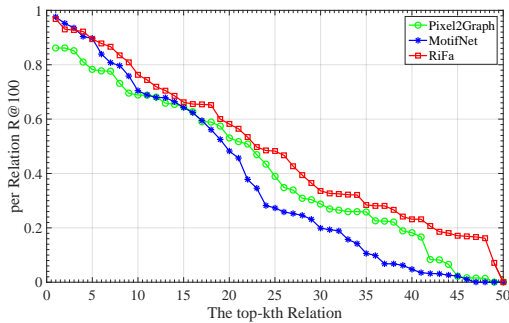


Figure 5. The per relation $R@100$ values of the 50 relations sorted in descendent order.

lutional neural network, which demonstrated the effectiveness of the proposed design principle.

For the future work, we shall further verify the generality of the design principle on other relation extraction models. The preliminary experiments in this paper already shown that many trained models did not actually capture the rich semantics of images. It is also very interesting to design metrics to evaluate the capability of each model on capturing different semantics and help explain which kind of semantics is captured in the generated scene graphs.

References

- [1] Martn Abadi, Ashish Agarwal, Paul Barham, Eugene Brevdo, Zhifeng Chen, Craig Citro, G.s Corrado, Andy Davis, Jeffrey Dean, Matthieu Devin, Sanjay Ghemawat, Ian Goodfellow, Andrew Harp, Geoffrey Irving, Michael Isard, Yangqing Jia, Rafal Jozefowicz, Lukasz Kaiser, Manjunath Kudlur, and Xiaoqiang Zheng. TensorFlow: Large-scale machine learning on heterogeneous distributed systems. In *OSDI 2016*, 03 2016.
- [2] Tianshui Chen, Weihao Yu, Riquan Chen, and Liang Lin. Knowledge-embedded routing network for scene graph generation. In *CVPR*, 2019.
- [3] Bo Dai, Yuqi Zhang, and Dahua Lin. Detecting visual relationships with deep relational networks. In *Proceedings of the IEEE Conference on Computer Vision and Pattern Recognition*, pages 3076–3086, 2017.
- [4] Kaiming He, Georgia Gkioxari, Piotr Dollr, and Ross Girshick. Mask R-CNN. In *CVPR 2017*, 2017.
- [5] Kaiming He, Xiangyu Zhang, Shaoqing Ren, and Jian Sun. Deep residual learning for image recognition. In *CVPR 2015*, 2015.
- [6] J. Johnson, R. Krishna, M. Stark, L. Li, D. A. Shamma, M. S. Bernstein, and L. Fei-Fei. Image retrieval using scene graphs. In *2015 IEEE Conference on Computer Vision and Pattern Recognition (CVPR)*, pages 3668–3678, June 2015.
- [7] Ranjay Krishna, Yuke Zhu, Oliver Groth, Justin Johnson, Kenji Hata, Joshua Kravitz, Stephanie Chen, Yannis Kalantidis, Li Jia Li, and David A. Shamma. Visual Genome: Connecting language and vision using crowdsourced dense image annotations. *International Journal of Computer Vision*, 123(1):32–73, 2017.
- [8] Yikang Li, Wanli Ouyang, Bolei Zhou, Jianping Shi, Chao Zhang, and Xiaogang Wang. Factorizable net: An efficient subgraph-based framework for scene graph generation. In *ECCV*, 2018.
- [9] Yikang Li, Wanli Ouyang, Bolei Zhou, Kun Wang, and Xiaogang Wang. Scene graph generation from objects, phrases and region captions. In *ICCV*, 2017.
- [10] Wentong Liao, Michael Ying Yang, Hanno Ackermann, and Bodo Rosenhahn. On support relations and semantic scene graphs. In *arXiv preprint arXiv:1609.05834*, 2016.
- [11] Tsung-Yi Lin, Piotr Dollr, Ross Girshick, Kaiming He, Bharath Hariharan, and Serge Belongie. Feature pyramid networks for object detection. In *CVPR 2017*, 2017.
- [12] Tsung-Yi Lin, Michael Maire, Serge Belongie, Lubomir Bourdev, Ross Girshick, James Hays, Pietro Perona, Deva Ramanan, C. Lawrence Zitnick, and Piotr Dollr. Microsoft COCO: Common objects in context. In *arXiv preprint arXiv:1405.0312*, 2015.
- [13] Cewu Lu, Ranjay Krishna, Michael Bernstein, and Li Fei-Fei. Visual relationship detection with language priors. In *European Conference on Computer Vision*, 2016.
- [14] Cewu Lu, Hao Su, Yongyi Lu, Li Yi, Chikeung Tang, and Leonidas Guibas. Beyond holistic object recognition: Enriching image understanding with part states. In *arXiv preprint arXiv:1612.07310*, 2016.
- [15] Alejandro Newell and Deng Jia. Pixels to graphs by associative embedding. In *NIPS 2017*, Long Beach, CA, USA, 2017.
- [16] Julia Peyre, Ivan Laptev, Cordelia Schmid, and Josef Sivic. Weakly-supervised learning of visual relations. In *ICCV*, 2017.
- [17] Francois Plesse, Alexandru Ginsca, Bertrand Delezoide, and Françoise Prêteux. Visual relationship detection based on guided proposals and semantic knowledge distillation. *ICME 2018*, 2018.
- [18] Bryan A Plummer, Arun Mallya, Christopher M Cervantes, Julia Hockenmaier, and Svetlana Lazebnik. Phrase localization and visual relationship detection with comprehensive linguistic cues. In *arXiv preprint arXiv:1611.06641*, 2016.
- [19] Mengshi Qi, Weijian Li, Zhengyuan Yang, Yunhong Wang, and Jiebo Luo. Attentive relational networks for mapping images to scene graphs. In *CVPR*, 2019.
- [20] Shaoqing Ren, Kaiming He, Ross Girshick, and Jian Sun. Faster R-CNN: Towards real-time object detection with region proposal networks. In *Advances in neural information processing systems*, 2015.
- [21] Wenbin Wang, Ruiping Wang, Shiguang Shan, and Xilin Chen. Exploring context and visual pattern of relationship for scene graph generation. In *CVPR*, 2019.
- [22] Danfei Xu, Yuke Zhu, Christopher Choy, and Li Fei-Fei. Scene graph generation by iterative message passing. In *Computer Vision and Pattern Recognition (CVPR)*, 2017.
- [23] Jianwei Yang, Jiasen Lu, Stefan Lee, Dhruv Batra, and Devi Parikh. Graph R-CNN for scene graph generation. In *ECCV*, 2018.
- [24] Rowan Zellers, Mark Yatskar, Sam Thomson, and Yejin Choi. Neural Motifs: Scene graph parsing with global context. In *Conference on Computer Vision and Pattern Recognition*, 2018.
- [25] Hanwang Zhang, Zawlin Kyaw, Jinyang Yu, and Shih-Fu Chang. PPR-FCN: Weakly supervised visual relation detection via parallel pairwise R-FCN. In *ICCV*, 2017.
- [26] Ji Zhang, Yannis Kalantidis, Marcus Rohrbach, Manohar Paluri, Ahmed Elgammal, and Mohamed Elhoseiny. Large-scale visual relationship understanding. In *2019 AAAI Conference on Artificial Intelligence (AAAI)*, Jan 2019.